# Report Weissinger

Luca Piomboni

December 13, 2023

**Abstract**

This project aims to conduct a comprehensive analysis of a three-dimensional problem, specifically focusing on the examination of a finite wing through the numerical implementation of Weissinger's method. The primary objective is to design a finite wing with the goal of minimizing induced drag while maintaining a fixed angle of attack and ensuring a specified range of values for $c_L$. The presence of a tail is also taken into account to reduce the wing pitching moment, both with and without the ground effect. The methodology has been developed using MATLAB, and its validation has been executed through XFLR5.

## 1 Introduction

The Weissinger's method is rooted in the Surface Panel Method theory, an aerodynamic approach employed for analyzing lift distribution on an aircraft wing's surface. This method entails subdividing the wing into small panels and calculating the lift on each of them. In the context of Weissinger's method, a key innovation involves considering the presence of a horseshoe vortex, strategically positioned at 1/4 of the chord length for each individual panel. By enforcing the non-penetration condition, a linear system can be solved to determine the circulation value for each panel. This information allows for deriving various critical parameters, including wing lift, induced drag, pitching moment, and the pressure coefficient for each panel, providing a comprehensive understanding of the aerodynamic behavior.

### 1.1 Objectives and expectations

The primary aim of this project is to develop a wing with a fixed angle of attack set at 2.6° and capable of achieving a lift coefficient ($C_L$) within the range of $0.3 \pm 0.05$, while concurrently minimizing induced drag. Subsequently, a tail has been introduced in the design, meticulously selected to minimize the pitching moment relative to the leading edge of the wing's root while maintaining the aforementioned $C_L$ for the wing. The analysis is finally extended to include ground effects in a subsequent iteration. All results are then compared and validated using XFLR5 software to ensure their consistency. It is relevant to note that, given the foundation of this approach in potential flow theory, viscous effects are not considered. Consequently, the only drag under consideration is the induced drag stemming from the wingtips. Therefore, the expectation is that to reduce the drag, the main element is the aspect ratio, since the limit for an infinite span wing is that the induced drag is zero, and the results are the same as for a single airfoil.

### 1.2 Computational apparatus

My computational apparatus is based on: CPU = Intel(R) Core(TM) i7-10510U CPU @1.80GHz RAM = 16GB Core used = 1 The clock time depend on the quantity of panels used, but the range is about [1,4] seconds for each single iteration.

## 2 Results

The results are obtained with a fixed wing angle of attack at 2.6°. I have chosen to keep dihedral and twist angles at zero, as the accuracy of these results is limited to small angles due to the exclusion of separation effects. To ensure an accurate representation, I have opted to maintain these parameters fixed while systematically varying the wing's aspect ratio and sweep angle. To achieve this, a comprehensive series of iterations was conducted, covering a wide range of values for these parameters across all three configurations (single, tandem, and with the ground).

## 2.1 Single airfoil

For the initial analysis, I examined the influence on the induced drag coefficient by first varying the aspect ratio, with a fixed chord of $3m$ and a variable wing span, while keeping $\Lambda = 0°$. I then set $AR = 7$, maintaining the same chord as before but changing the values of the sweep angle. Throughout this investigation, the angle of attack was kept at 2.6°, and the other setups not mentioned can be taken from Table 1. The findings from this analysis reveal that as the aspect ratio rises, the induced drag increases. This behavior disagrees completely with the initial expectations. Regarding the dependence of induced drag on the sweep angle, the results show that drag decreases as the sweep angle increases. Based on what was obtained before, this may not represent a consistent result and is probably due to some bugs in the code for evaluating the aerodynamic coefficients. The graphical representation of these results is depicted in Figure 3.

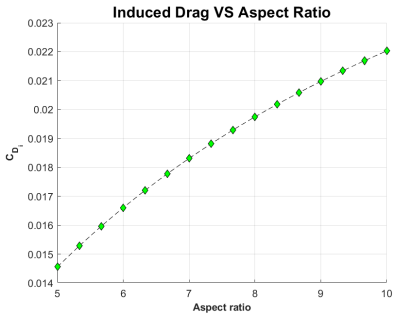


(a) Induced drag function of the aspect ratio.

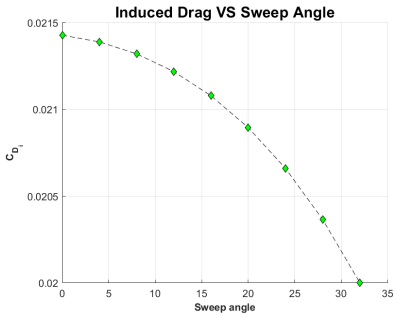


(b) Induced drag function of the sweep angle.

Figure 1: Dependence of the induced drag coefficient on the wing design.

Besides the results, to continue with the project's objective, I decided to consider a wing with an aspect ratio that can be both real and effectively meet the requirements, with $\Lambda = 20°$. This wing design will be maintained in the subsequent configurations when referring to the wing, and the setups used are detailed in Table 1. Despite the unfavorable results for drag, the values of the pressure and lift coefficients appear to be correct, as well as for the circulation gamma. This can be observed in Figure 2 and Table 2.

| $u_\infty$ [m/s] | $\alpha$ [°] | $\beta$ [°] | $\rho$ $[kg/m^3]$ | $c_w$ [m] | $span_w$ [m] | $\Lambda_w$ [°] | $d_w$ [°] | $N_{c,w}$ | $N_{s,w}$ |
|---|---|---|---|---|---|---|---|---|---|
| 1 | 2.6 | 0 | 1.225 | 3 | 21 | 20 | 0 | 20 | 40 |

Table 1: Data-set single wing.

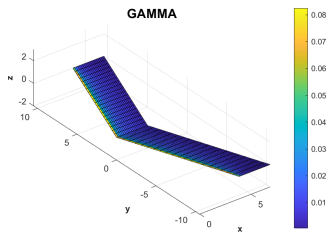


(a) Circulation distribution.

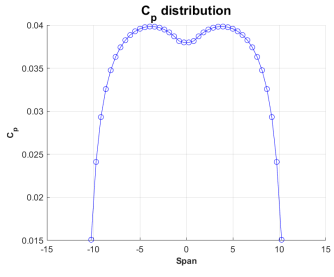


(b) Pressure coefficient at 1/4 of the chord.

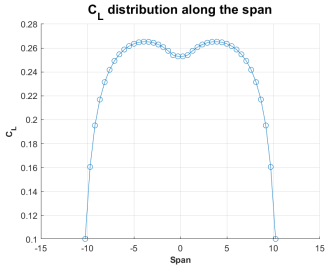


(c) Lift coefficient at 1/4 of the chord.

Figure 2: Results for the simulation of a single wing.

| $C_L$ | $C_{D_i}$ | $C_M$ |
|---|---|---|
| 0.1953 | 0.0183 | -0.1652 |

Table 2: Aerodynamic coefficients obtained.

## 2.2 Tandem configuration

I am now going to provide the results for the tail design to reduce the pitching moment of the front wing defined previously. To do so, once again, I changed the values of the tail span, keeping the chord at $1.5m$ and $\Lambda = 0°$. The distance in the x-direction between the leading edge of the tail and the wing is set at $5m$, while their difference in height is $0.5m$, with the tail above the wing. The results in Figure 3a show that an increase in the aspect ratio leads to an increase in the pitching moment with respect to the leading edge. This is consistent with expectations, as an increase in the lift coefficient will correspond to an increase in the pitching moment.

Regarding the aspect ratio dependence, the same wing-tail distances have been considered, and for the tail design, the same chord and a low value of the aspect ratio are adopted, with the span set at $6m$. The findings in Figure 3b show that as $\Lambda$ increases, the pitching moment decreases."

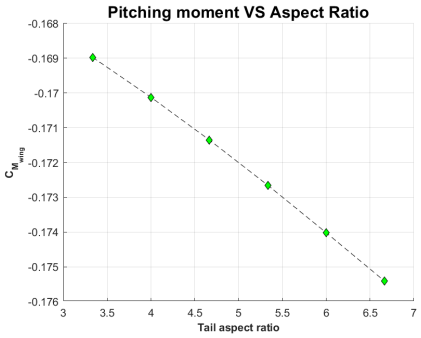


(a) Pitching moment coefficient VS tail aspect ratio.

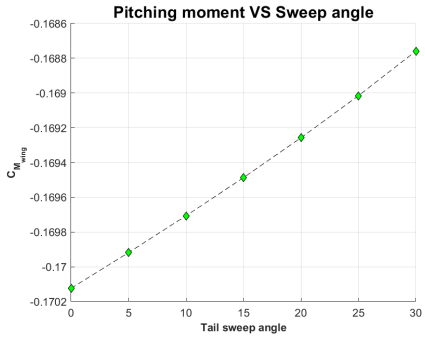


(b) Pitching moment coefficient VS tail sweep angle.

Figure 3: Dependence of the wing pitching moment on the tail design.

Accounting for these results I decided to design a tail which specifications are provided in Table 3. Therefore, considering the very same wing design before, I evaluated the value of the circulation on each panel and all the fluid parameters that are shown in Figure 4 and Table 4.

| $u_\infty$ [m/s] | $\alpha$ [°] | $\beta$ [°] | $\rho$ $[kg/m^3]$ | $c_t$ [m] | $span_t$ [m] | $\Lambda_t$ [°] | $d_t$ [°] | $x_{wt}$ | $h_{wt}$ | $N_{c,t}$ | $N_{s,t}$ |
|---|---|---|---|---|---|---|---|---|---|---|---|
| 1 | 2.6 | 0 | 1.225 | 1.5 | 6 | 30 | 0 | 5 | 0.5 | 20 | 40 |

Table 3: Data-set single wing

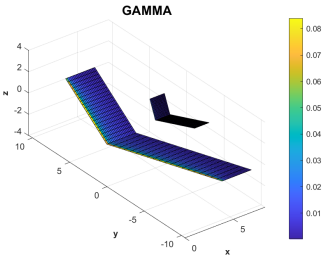


(a) Gamma distribution.

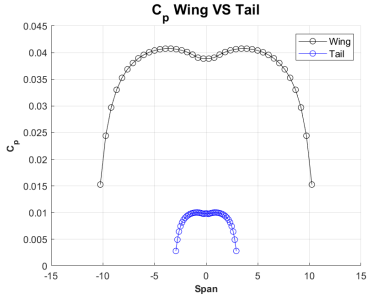


(b) Pressure distribution at $c/4$

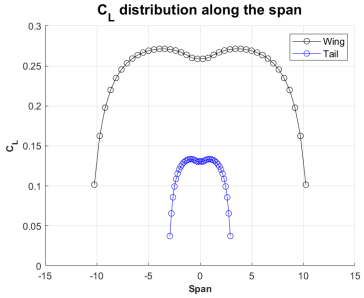


(c) Lift distribution at $c/4$

Figure 4: Results for the simulation of tandem configuration.

| $C_{L_{wing}}$ | $C_{D_{i_{wing}}}$ | $C_{M_{wing}}$ | $C_{L_{tail}}$ | $C_{D_{i_{tail}}}$ | $C_{M_{tail}}$ |
|---|---|---|---|---|---|
| 0.1995 | 0.0218 | -0.1688 | 0.0954 | -0.0043 | -0.0746 |

Table 4: Aerodynamics coefficients obtained.

## 2.3 Ground effect

As a final step, I added the effect of the ground to observe its impact on the aerodynamic coefficients. The settings for the tail and the wing remain the same as provided in Tables 1 and 3, while the altitude of the first wing is $0.5m$ from the ground. A comparison between the data obtained in this configuration and the one without the ground (Figure 4) has been provided for a comprehensive representation of the results shown in all the figures below.

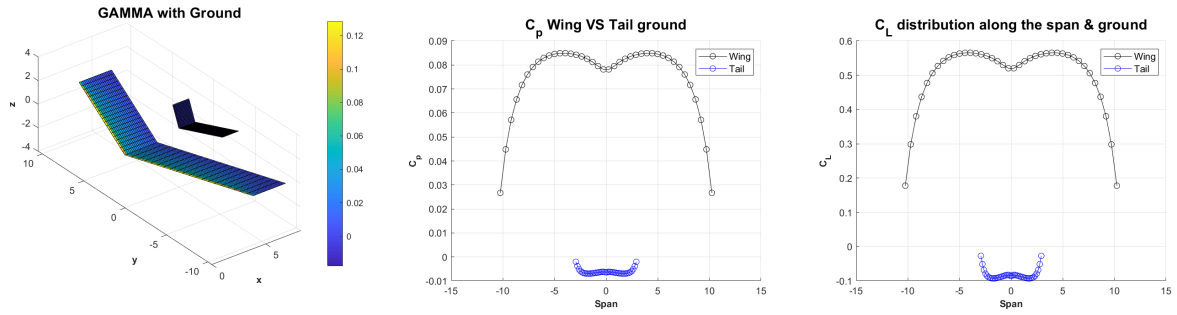


(a) Gamma distribution in ground proximity.

(b) Pressure coefficient at $c/4$.

(c) Lift coefficient at $c/4$.

Figure 5: Results for the simulation of tandem configuration and ground proximity.

I also conducted an analysis of the dependence of the drag and lift coefficients on the distance from the ground, and the results are presented in Figure 6.

| $C_{L_{wing}}$ | $C_{D_{i_{wing}}}$ | $C_{M_{wing}}$ |
|---|---|---|
| 0.1995 | 0.0218 | -0.1688 |
| $C_{L_{tail}}$ | $C_{D_{i_{tail}}}$ | $C_{M_{tail}}$ |
| 0.0954 | -0.0043 | -0.0746 |

Table 5: Aerodynamics coefficients obtained.

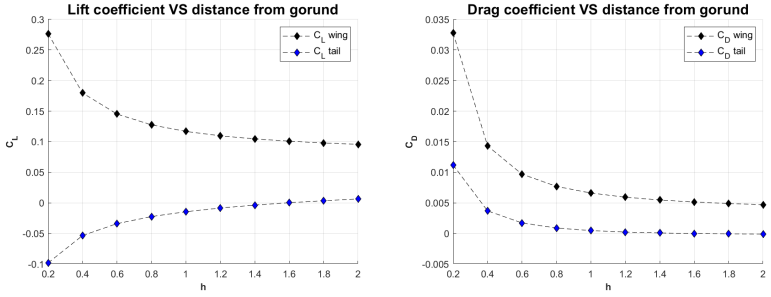


Figure 6: Aerodynamics coefficients dependence on the ground proximity.

# 3 Validation and post processing

For the validation and post-process analysis, I used both XFLR5 software and the data provided in the project materials to compare the results. When examining the results, we must consider that the data taken from the lab materials are obtained through graphical estimation, introducing slight errors. The values are intended solely for understanding the overall correctness of the curve's shape. This approach serves the dual purpose of facilitating a more in-depth comparison (since XFLR5 does not provide the values of the gamma distribution on each panel) and understanding where errors may occur in the evaluation of the drag coefficient. For this purpose I evaluated the correctness of the results on a single wing (which setup is provided in Table 7), since the code work in the same way basically also for the other two configurations, performing only more iterations. Form the results provided in Figure 8 it is possible to see that both the results for the circulation gamma (where is only reported the values for the panels that are on the leading edge) and pressure coefficient are perfectly aligned with the expectations.

| $u_\infty$ [m/s] | $\alpha$ [°] | $\beta$ [°] | $\rho$ $[kg/m^3]$ | $c_w$ [m] | $span_w$ [m] | $\Lambda_w$ [°] | $d_w$ [°] | $N_{c,w}$ | $N_{s,w}$ |
|---|---|---|---|---|---|---|---|---|---|
| 1 | 3 | 0 | 1 | 3 | 18 | 0 | 0 | 20 | 40 |

Table 6: Data-set for validation.

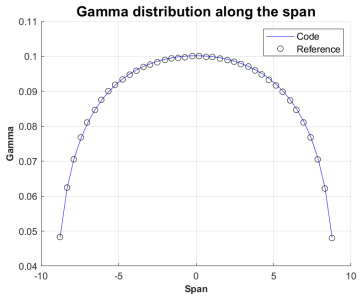


(a) Comparison of gamma distribution on the leading edge.

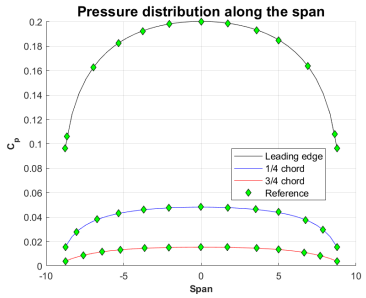


(b) Comparison pressure coefficient distribution.

Figure 8: Results comparison for validation.

| Software | $C_{L_{wing}}$ | $C_{D_{i_{wing}}}$ | $C_{M_{wing}}$ |
|---|---|---|---|
| MATLAB | 0.2238 | 0.0258 | -0.0563 |
| XFLR5 | 0.224 | 0.012 | -0.054 |

Table 7: Aerodynamic coefficients comparison.

The same cannot be said for the lift and drag coefficients. Regarding lift, its value slightly differs from the expectations (Figure 10), while for drag, I observed a completely opposite behavior than what is anticipated, as shown in Figure 9. The curve, in fact, should exhibit a minimum at the wing root and a maximum at the tips, given that we're dealing with induced drag. The notion is that there might be an error in their evaluation, and with high probability, the error lies in the formula used or its implementation. Finally, since the pitching moment is obtained from the previous two load components, its values must be incorrect as well.

Further work is needed to fix this minor bug, which appears to be limited to a small part of the code. Nevertheless, the overall implementation seems to correctly predict the actual results.

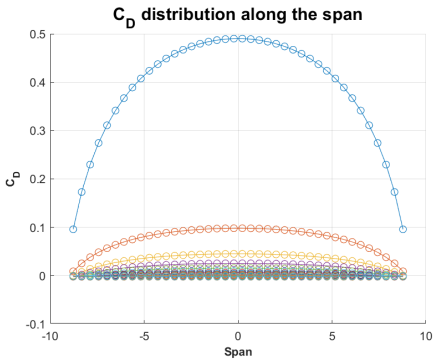


Figure 9: Induced drag results obtained with the implemented code.

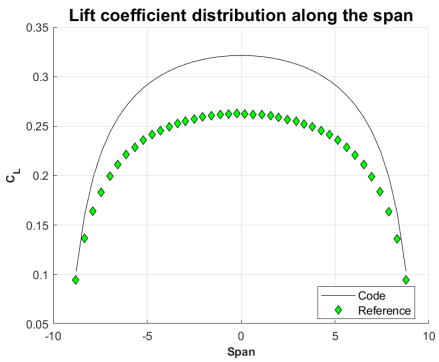


Figure 10: Lift coefficient comparison with the professor's results.

# 4 Conclusion

This study has led to the conclusion that the implemented method is capable of generating favorable results for the distribution of circulation across all panels. However, a discrepancy arises due to an issue in the final segment of the code responsible for evaluating aerodynamic loads, where their values deviate from expectations. Following an in-depth analysis of the code and a thorough discussion of the obtained results, it appears that the error may be traced back to the function responsible for evaluating aerodynamic loads, stemming from a wrong implementation of the specific formula in the code.

Notwithstanding this minor setback, which should require minimal effort to rectify, the remainder of the code reliably provides optimal data. Although the overall results obtained do not currently meet the required lift coefficient, once the code is fixed, the process can be readily repeated to ensure accurate alignment with the specified requirements.